CONTAINMENT RECIRCULATION SUMP HYDRAULIC PERFORMANCE

STANDARDIZED NUCLEAR UNIT POWER PLANT SYSTEM (SNUPPS)

by
James B. Nystrom

Prepared for
SNUPPS Nuclear Power Plants

ALDEN RESEARCH LABORATORY
WORCESTER POLYTECHNIC INSTITUTE

30-83/M458F

March 1983

CONTAINMENT RECIRCULATION SUMP HYDRAULIC PERFORMANCE
STANDARDIZED NUCLEAR UNIT POWER PLANT SYSTEM (SNUPPS)

by

James B. Nystrom

Prepared for

SNUPPS Nuclear Power Plants

George E. Hecker, Director

ALDEN RESEARCH LABORATORY

WORCESTER POLYTECHNIC INSTITUTE

HOLDEN, MASSACHUSETTS

March 1983

ABSTRACT

A hydraulic model of the two containment recirculation sumps for the Standardized Nuclear Unit Power Plant System (SNUPPS) was constructed at a scale of 1:2.98. To assure acceptable sump performance, the model was tested for a variety of possible approach flow distributions, bar rack and screen blockages, water levels, and pump operation combinations. The tests were designed to assure that no air entraining vortices would be formed, to determine that head losses across the screens and in the pipe inlets are acceptable, and to assure acceptable values for swirl in the inlet pipes.

Initial tests of the original design indicated air core vortices could form with some approach flow distributions and some sump screen blockage configurations. Therefore, a vortex suppression device was designed and installed in the model, consisting of a floor grating placed horizontally over the entire top of the sumps.

Tests with the vortex suppressor in place indicated the maximum strength vortex was a surface dimple, even when the model was operated at velocities above scaled design conditions as a check on possible model scale effects.

With the vortex suppression device installed, the maximum swirl angle measured was 1.6 degrees for the containment spray (CS) pump suction line. Typical swirl angles were considerably lower, less than one degree. These magnitudes of swirl angles were on the order of what would be expected from a single bend and were, therefore, not of practical significance. The measured inlet loss coefficient included the screen losses and the vortex suppression device. The inlet loss coefficient was about 0.35, based on the area average pipe velocity head, with 50 percent screen blockage.

The sump design with the vortex suppressor installed was found to have acceptable hydraulic performance for all operating conditions.

TABLE OF CONTENTS

INTRODUCTION

The Standardized Nuclear Unit Power Plant System (SNUPPS) is a 1150 MWe pressurized water reactor. Two plants are under construction: Wolf Creek and Callaway. The nuclear-safety-related containment recirculation sumps are designed to supply the containment spray system (CS) and the residual heat removal (RHR) system with water during the recirculation mode. For a Loss of Coolant Accident (LOCA), the containment spray system is designed to depressurize the containment building and the residual heat removal system is designed to provide cooling to the core. During initial operation of the safety injection system, water from the refueling water storage tank (RWST) is injected into the core and sprayed throughout the containment via the RHR and CS systems, respectively. The containment recirculation sumps collect water spilling onto the containment floor. The two RHR pumps begin to take suction from the sump when the switchover process from the RWST is complete. The water level in the containment at this time is estimated to be at elevation 2002 ft 4 inches (29)*. To provide core cooling in the recirculation mode, the water flows through recirculation coolers and is delivered to the reactor. The two containment spray pumps are also supplied from the recirculation sumps once the RWST has drained to a preset level and switchover is completed. The water level in the containment at this time is estimated to be at elevation 2003 ft 6-1/2 inches (29).

The containment recirculation sumps must not have any adverse hydraulic performance characteristics which might degrade their ability to perform their design function. The Alden Research Laboratory (ARL) of Worcester Polytechnic Institute (WPI) was authorized by Nuclear Projects Incorporated, an agent for the SNUPPS Utilities, to construct and test a model of the SNUPPS containment recirculation sumps. The objectives were to investigate the potential for free surface vortex formation and swirl in the inlet piping, determine if inlet losses were within acceptable limits and evaluate if any other flow conditions could adversely affect the performance of the containment spray pumps or residual heat removal pumps in the recirculation mode.

*( ) Typically denotes reference

Vortex formation may lead to air ingestion which may degrade pump performance. Likewise, high swirl angles (solid body flow rotation) in the suction pipes may be detrimental to pump performance. To assure conservative design, a vortex strength greater than a coherent dye core (type 3) and swirl angles greater than five degrees were considered unacceptable hydraulic performance. Vortex strengths are shown in Figure 11 and swirl angle is defined by Equation 14. Operating conditions involving various possible water levels; pump operation combinations; approach flow distributions; blockages of gratings, coarse screens and, fine screens; and combinations thereof were tested in the model.

This report presents the findings of the study and includes a description of the prototype and the model, and summarizes conditions investigated, similitude considerations, test procedures, instrumentation, and interpretation of results.

PROTOTYPE DESCRIPTION

The SNUPPS containment recirculation sumps are located adjacent to the secondary shield wall at elevation 2000 ft 0 inches as shown in Figure 1. The sumps are adjacent, separated by a concrete wall, and are eight ft square and eight ft deep. Figure 2 shows a cross-section of the reactor containment building and indicates major equipment locations. The sumps are protected from direct water jet or missile impingement by the secondary shield wall and a concrete platform supporting the accumulator.

A CS pump and an RHR pump suction pipe exit each sump horizontally at elevation 1994 ft. The CS and RHR suction pipes have 12 and 13.5 inch IDs, respectively. Each pipe inlet includes a conical bellmouth having a cross vane swirl suppressor.

Each containment recirculation sump is protected from debris ingestion by the three stage vertical screen system shown in Figure 3. The coarsest debris is removed by an outer trashrack having bearing bars 2 inch by 3/16 inch on 19/16 inch centers. Two inner sets of screens, each mounted on a trashrack, remove fine debris. The trashrack and screens are about eight ft high. A six inch high concrete curb surrounds each sump to eliminate high density trash.

Upon realignment to the recirculation mode, the RHR pumps will draw water from the sumps at a minimum water level of 2002 ft 4 inches. The CS pumps will continue to draw water from the RWST until the low-low-2 tank level alarm, at which time they will be aligned to the recirculation mode. The minimum water level at this time is calculated to be elevation 2003 ft 6-1/2 inches. During recirculation the RHR and CS pumps operate with the design flowrates given in Table 1.

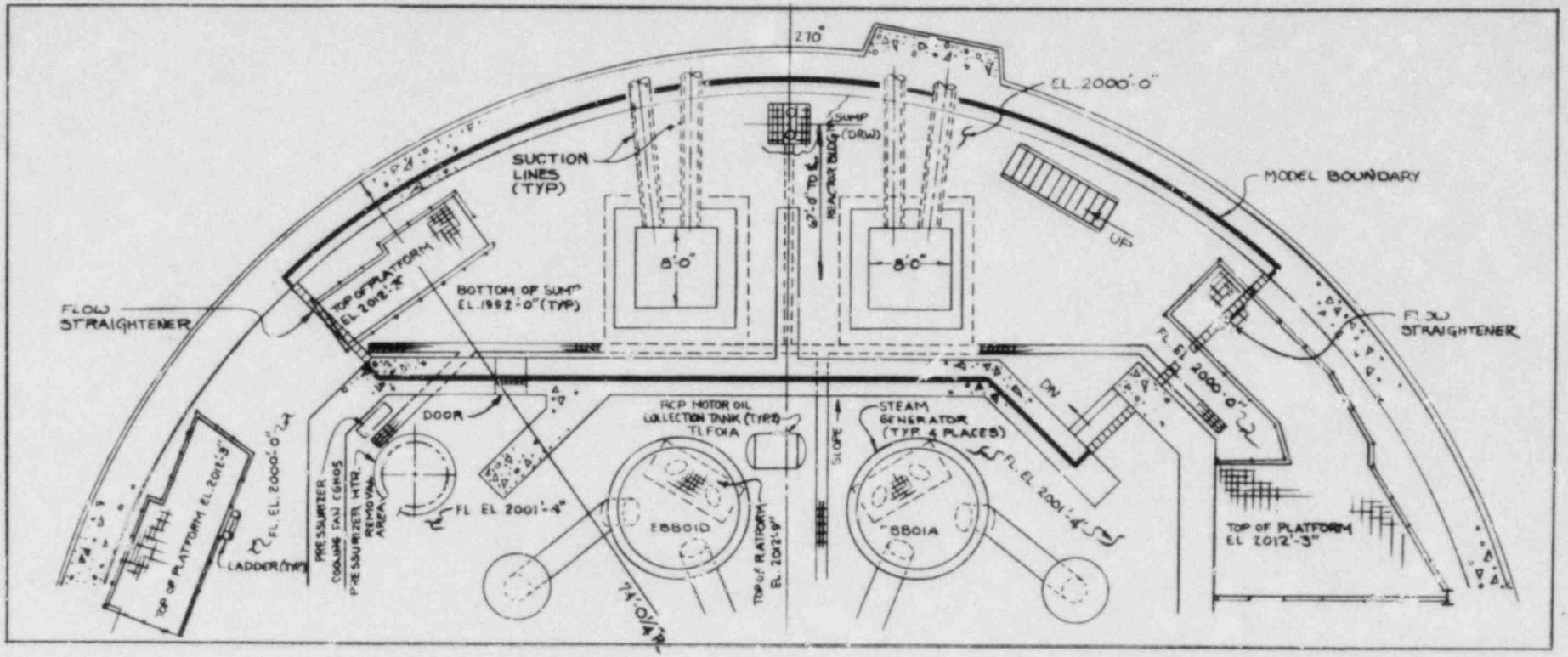

FIGURE 1 PARTIAL PLAN OF REACTOR CONTAINMENT BUILDING IN THE AREA OF THE CONTAINMENT SUMPS

ARL

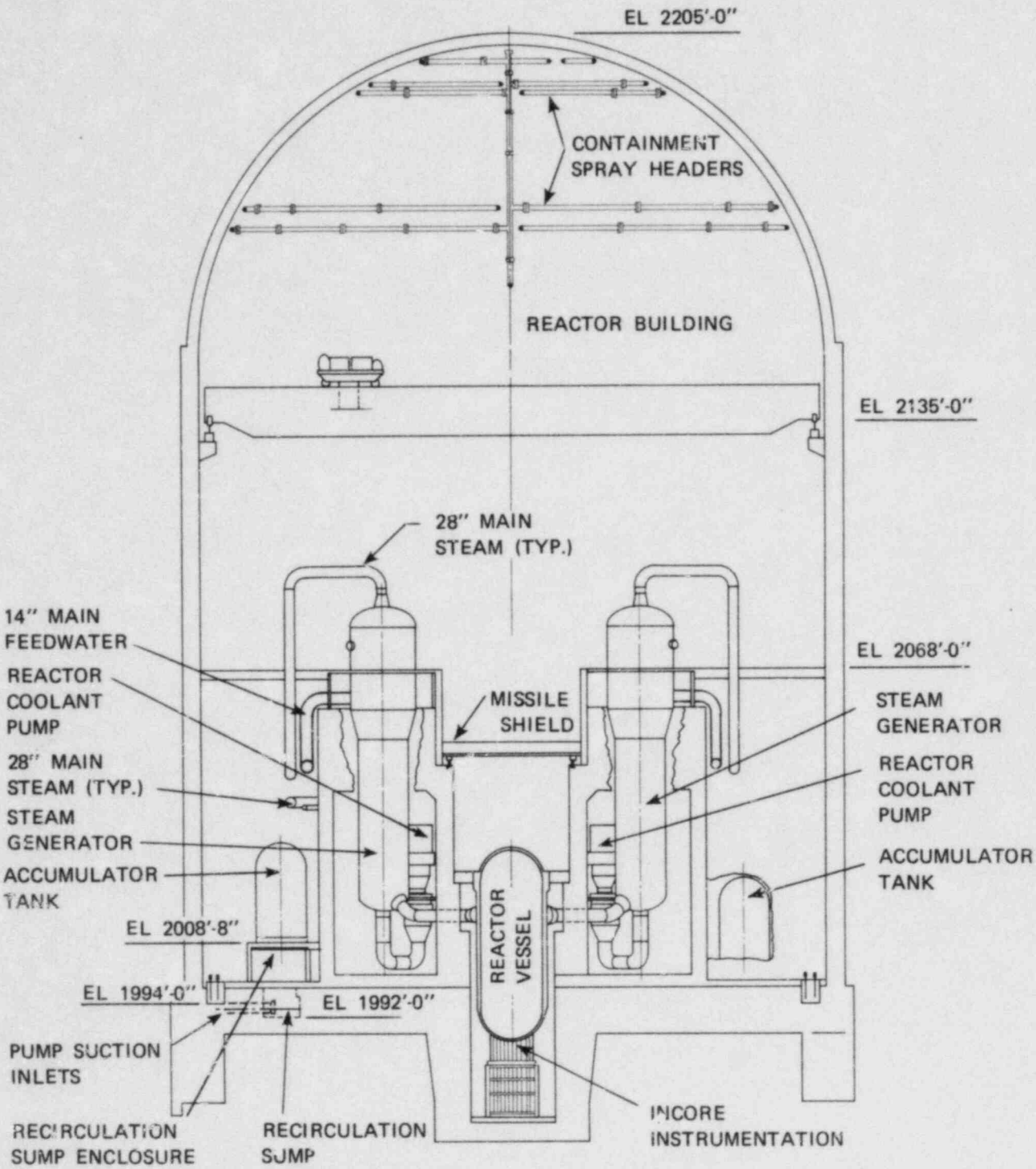

FIGURE 2 CROSS-SECTION OF REACTOR BUILDING INDICATING LOCATION OF RECIRCULATION SUMPS RELATIVE TO MAJOR EQUIPMENT

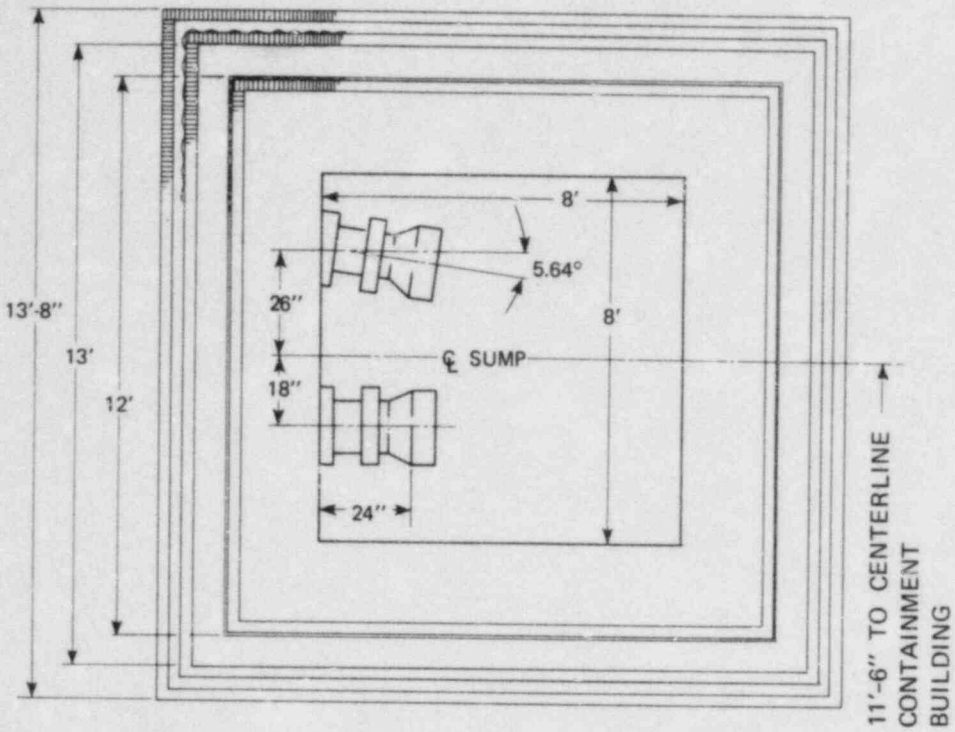

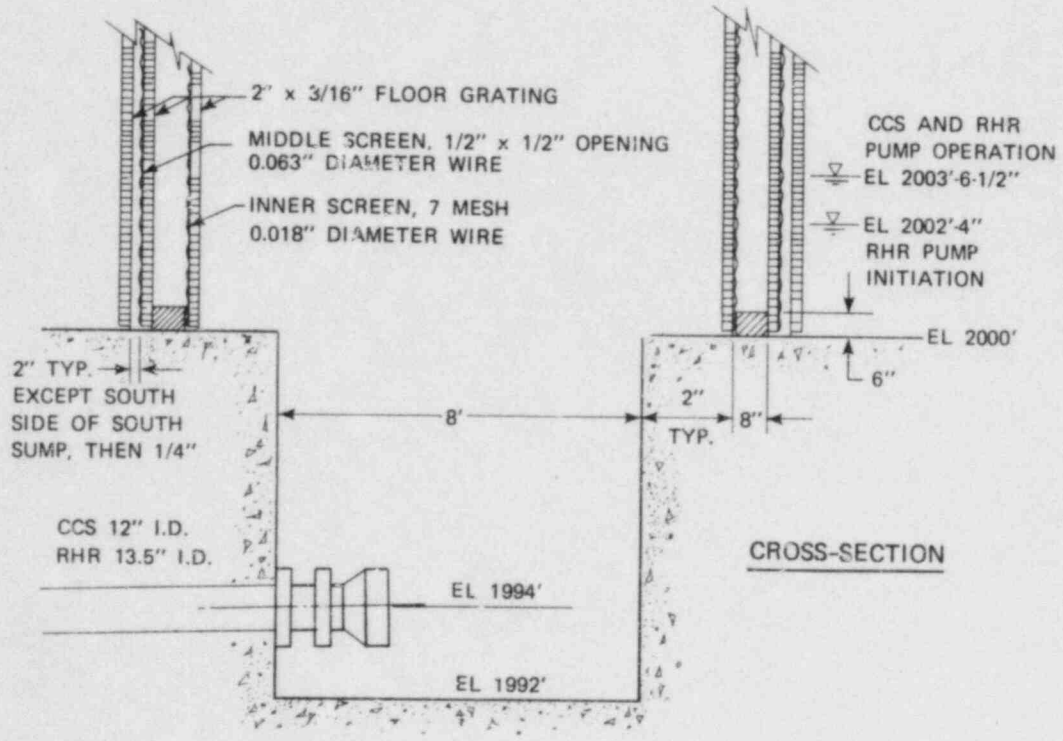

FIGURE 3 CROSS-SECTION OF CONTAINMENT RECIRCULATION SUMP AND SCREEN SYSTEM

TABLE 1

Design Pump Flowrates (gpm)

for Containment Recirculation Sumps

Water Level	RHR	CS
2002 ft 4 inches	4800	0
2003 ft 6 1/2 inches	4850	3950

A visit by ARL personnel to the engineering scale model was conducted to assure the interpretation and completeness of drawings in regard to the primary approach flow patterns, possible secondary flow paths, and the various equipment obstructing the flowpaths.

Major equipment with diameters greater than three inches were considered relevant in possible influence of flow conditions. Research (26) has shown that obstructions with dimensions of 12 to 24 inches (prototype) do not measurably affect key sump performance parameters. Therefore, modeling equipment with 3 inch diameters is a conservative criterion. Photographic documentation during the model visit allowed details to be checked as model design proceeded.

SIMILITUDE

The study of dynamically similar fluid motions forms the basis for the design of models and the interpretation of experimental data. The basic concept of dynamic similarity may be stated as the requirement that two systems with geometrically similar boundaries have geometrically similar flow patterns at corresponding instants of time (3). Thus, all individual forces acting on corresponding fluid elements of mass must have the same ratios in the two systems.

The conditions required for complete similitude may be developed from Newton's second law of motion:

$$F_i = F_p + F_g + F_v + F_t \qquad (1)$$

where

F_i = inertia forces, defined as mass, M, times the acceleration, a
F_p = pressure force connected with or resulting from the motion
F_g = gravitational force
F_v = viscous force
F_t = force due to surface tension

Additional forces may be relevant under special circumstances, such as fluid elasticity, magnetic or Coriolis forces, but these had no influence on this study and were, therefore, not considered in the following development.

Two systems which are geometrically similar are dynamically similar if both satisfy the dimensionless form of the equation of motion. Equation (1) can be made dimensionless by dividing all the terms by F_i. Rewriting each of the forces of Equation (1) as:

F_p = net pressure x area = $\alpha_1 \Delta p L^2$

F_g = specific weight x volume = $\alpha_2 \gamma L^3$

F_v = shear stress x area = $\alpha_3 \mu \Delta u/\Delta L$ x area = $\alpha_3 \mu u L$

F_t = surface tension x length = $\alpha_4 \sigma L$

F_i = density x volume x acceleration = $\alpha_5 \rho L^3 u^2/L = \alpha_5 \rho u^2 L^2$

where

α_1 α_2, etc. = proportionality factors

L = representative linear dimension

p = net pressure

γ = specific weight

μ = dynamic viscosity

σ = surface tension

ρ = density

u = representative velocity

Substituting the above terms in Equation (1) and making it dimensionless by dividing by the inertial force, F_i, we obtain

$$\frac{\alpha_1}{\alpha_5} E^{-2} + \frac{\alpha_2}{\alpha_5} F^{-2} + \frac{\alpha_3}{\alpha_5} R^{-1} + \frac{\alpha_4}{\alpha_5} W^{-2} = 1 \qquad (2)$$

where

$$E = \frac{u}{\sqrt{\Delta p/\rho}} = \text{Euler number; } \frac{\text{Inertia Force}}{\text{Pressure Force}}$$

$$F = \frac{u}{\sqrt{gL}} = \text{Froude number; } \frac{\text{Inertia Force}}{\text{Gravity Force}}$$

$$R = \frac{u\,L}{\mu/\rho} = \text{Reynolds number; } \frac{\text{Inertia Force}}{\text{Viscous Force}}$$

$$W = \frac{u}{\sqrt{\sigma/\rho L}} = \text{Weber number; } \frac{\text{Inertia Force}}{\text{Surface Tension Force}}$$

Since the proportionality factors, α_i, are the same in model and prototype, complete dynamic similarity is achieved if all the dimensionless groups, E, F, R, and W, have the same values in model and prototype. In practice, this is difficult to achieve. For example, to have the values of F and R the same requires either a 1:1 full scale model or a fluid of very low kinematic viscosity in the reduced scale model. Hence, the accepted approach is to select the predominant forces and design the model according to the appropriate dimensionless group. The influence of the other forces would be secondary and are called scale effects (2, 3).

Froude Scaling

Models involving a free surface are constructed and operated using Froude similarity since the flow process is controlled by gravity and inertia forces. The Froude number, representing the ratio of inertia to gravitational force,

$$F = u/\sqrt{gs} \qquad (3)$$

where

u = average velocity
g = gravitational acceleration
s = submergence, the representative linear dimension

was, therefore, made equal in model and prototype.

$$F_r = F_m/F_p = 1 \quad (4)$$

In modeling an intake sump to study the formation of vortices, it is important to select a reasonably large geometric scale to achieve large Reynolds numbers and to reproduce the curved flow pattern in the vicinity of the intake (4). At sufficiently high Reynolds number, an asymptotic behavior of energy loss coefficients with Reynolds number is usually observed (2). Hence, with F_r = 1, the basic Froudian scaling criterion, the Euler numbers, E, will be equal in model and prototype. This implies that flow patterns and loss coefficients are equal in model and prototype at sufficiently high Reynolds numbers. A geometric scale of $L_r = L_m/L_p = 1/2.98$ was chosen for the model, where L refers to length. From Equations (3) and (4), using $s_r = L_r$, the velocity, discharge, and time scales were:

$$u_r = L_r^{0.5} = 1/\sqrt{2.98} = 1/1.73 \quad (5)$$

$$Q_r = L_r^2 u_r = L_r^{2.5} = 1/(2.98)^{2.5} = 1/15.34 \quad (6)$$

$$t_r = L_r^{0.5} = 1/\sqrt{2.98} = 1/1.73 \quad (7)$$

Similarity of Vortex Motion

Fluid motions involving vortex formation in sumps of low head pump intakes have been studied by several investigators (1, 4, 5, 6).

It was found that viscous and surface tension forces could influence the formation and strength of vortices (1, 5). The relative magnitude of these

forces on the fluid inertia force is reflected in the Reynolds and Weber numbers, respectively, which are defined as:

$$R = u\, d/\nu \tag{8}$$

$$W = \frac{u}{(\sigma/\rho r)^{1/2}} \tag{9}$$

where r = characteristic radius of vortex and d = intake diameter. It was important for this study to ascertain any deviations in similitude attributable to viscous and surface tension forces in the interpretation of model results. For large R and W, the effect of viscous and surface tension are minimal, i.e., inertial forces predominate. Surface tension effects are negligible when r is large, which will be true for weak vortices where the free surface is essentially flat. Conversely, only strong air-core vortices are subject to surface tension scale effects. Moreover, an investigation using liquids of the same viscosity but different surface tension coefficients ($\sigma = 4.9 \times 10^{3}$ lb/ft to 1.6×10^{3} lb/ft) showed practically no effect of surface tension forces on the vortex flow (1). The vortex severity, S, is therefore mainly a function of the Froude number, but could also be influenced by the Reynolds number.

$$S = S\ (F,\ R) \tag{10}$$

Anwar (4) has shown by principles of dimensional analysis that the dynamic similarity of fluid motion in an intake is governed by the dimensionless parameters given by

$$\frac{4Q}{u_\theta\, d^2}\ ,\ \frac{u}{\sqrt{2gs}}\ ,\ \frac{Q}{\nu\ s}\ ,\ \text{and}\ \frac{d}{2s}$$

where

Q = discharge through the outlet

u_θ = tangential velocity at a radius equal to that of outlet pipe

d = diameter of the outlet pipe

Surface tension effects were neglected in his analysis, being negligible for weak vortices. The influence of viscous effects was defined by the parameter $Q/(\nu\ s)$, known as a radial Reynolds number, R_R.

For similarity between the dimensions of a vortex of strengths up to and including a narrow air-core type, it was shown that the influence of R_R becomes negligible if $Q/(\nu\ s)$ was greater than 3×10^4 (4). As strong air-core type vortices, if present in the model, would have to be eliminated by modified sump design, the main concern for interpretation of prototype performance based on the model performance would be on the similarity of weaker vortices, such as surface dimples and dye-cores. In the model for Froude scale velocity and for water temperatures of 60°F, the values of R_R was greater than 3×10^4 for all operating conditions. Thus, viscous forces would have only a secondary role in the present study. Dynamic similarity is obtained by equalizing the parameters $4Q/u_\theta d^2$, $u/\sqrt{2gs}$, and $d/2s$ in model and prototype. A Froudian model would satisfy this condition.

To compensate for any possible excessive viscous energy dissipation and consequently less intense model vortex, various investigators have proposed increasing the model flow and, therefore, the approach and intake velocity, since the submergence is maintained constant. Operating the model at the prototype inlet velocity (pipe velocity) is believed by some researchers to achieve the desired results (1). This is often referred to as the Equal Velocity Rule, and is considered to give conservative predictions of prototype performance. The test procedure for the present study incorporated testing the model at prototype pipe velocities to achieve conservative predictions.

ARL has conducted an extensive research program to assure that the conclusions regarding the effect of Reynolds number on vortex activity in the model are valid for the prototype. A technique of extrapolating model vortex activity to prototype Reynolds numbers (12) by using elevated model water temperatures (up to 165°F) and varying model flow velocity (Froude ratio) has been applied to several studies (11, 13, 14, 19, 26). Figure 4 illustrates the method used to investigate scale effects and predict vortex types in the prototype based on model results (12). The ordinate, F_r, is the ratio of model to prototype Froude number, while the abscissa is the inlet pipe Reynolds number, R. The objective is to determine flow conditions at $F_r = 1$ at prototype R from tests at lower than prototype R. Assume the model to operate at flow less than Froude scaling ($F_r < 1$) at point a_1. By increasing the discharge in the model while keeping the same submergence and temperature, F_r and R are increased corresponding to a point, a_N, where a vortex of type N was first observed. The model Reynolds number can also be changed by varying the kinematic viscosity with temperature changes, and similar tests performed to locate b_N, another point on the locus of type N vortices. Extrapolation of the line of constant vortex strength of type N can be made to a prototype Reynolds number at the proper Froude number ($F_r = 1$), point P_N. The locus could represent any expedient measure of vortex severity. Any scale effects due to viscous forces would be evaluated and taken into account by such a projection procedure. The high temperature high flow tests were used in the similar fashion for projecting the inlet loss coefficients (from pressure gradeline measurements) and swirl severities (from vortimeter readings) over a wide range of Reynolds and Froude numbers.

Figure 5 shows the results of one recirculation sump model (14) which are typical of the other four studies conducted. As can be seen from the data, which are for the final design with vortex suppressor grids, there are no measurable changes in vortex strength with Reynolds number. This is reasonable since the Reynolds numbers are all above the limiting value (1, 4), a previously described similitude requirement. Minor increases in vortex strength occur when the Froude ratio is increased. Other measurements, such

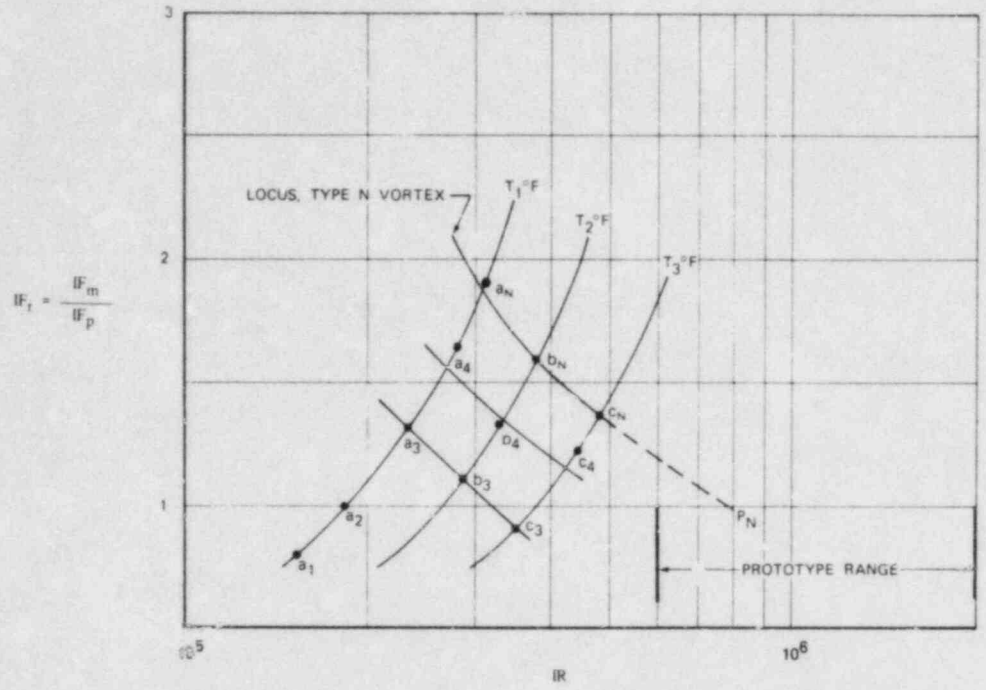

FIGURE 4 ARL VORTEX ACTIVITY EXTRAPOLATION TECHNIQUE

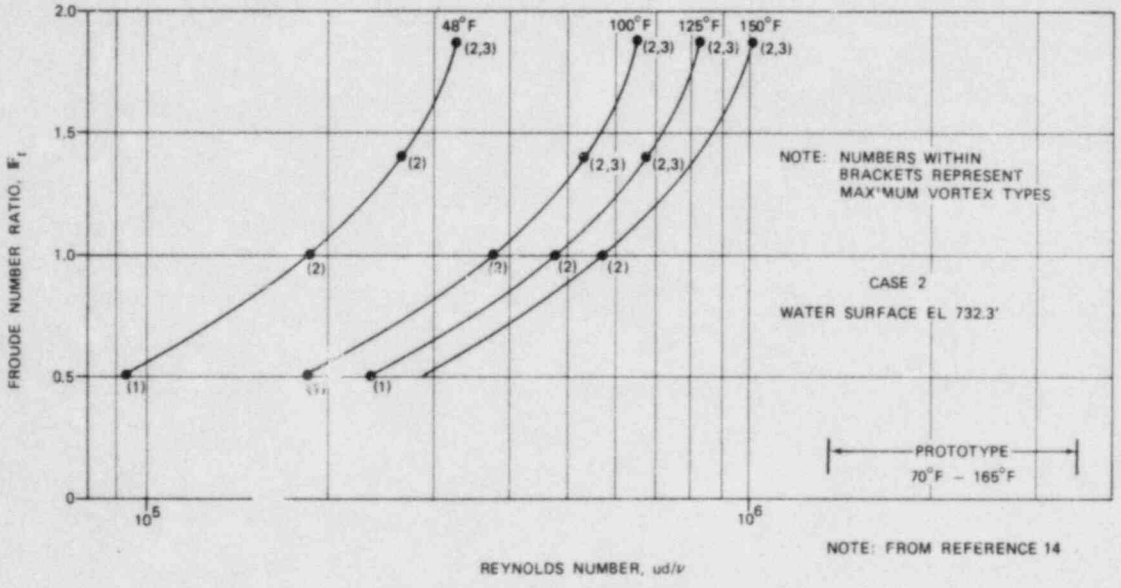

FIGURE 5 TYPICAL MODEL RESULTS FOR ARL VORTEX ACTIVITY EXTRAPOLATION TECHNIQUE

as swirl in the inlet pipe, have also shown no measurable dependence on Reynolds number. This indicates that reduced scale model tests at Froude scaled flow (i.e., $F_r = 1$) are a direct indication of prototype performance for weak vortices, particularly if vortex suppressors are part of the design Tests at higher than Froude scale flow are seen to give conservative results, i.e., somewhat stronger vortices than expected in the prototype. Since for this study the minimum Reynolds number is comparable to the minimum for the previous studies which indicated no increase in vortex activity for increasing Reynolds numbers at constant Froude ratio, it is concluded that no scale effects will be present in the model and tests at temperatures greater than ambient are not required.

Based on a review of information on model versus prototype vortices for comparable conditions, Hecker (23) concluded that there are negligible scale effects for weak vortices, and that only a relatively small increase in the model flow rate is necessary to overcome the secondary scale effects for strong vortices.

A portion of a parametric study of containment sumps conducted for the NRC was specifically designed to investigate the possibility of scale effects when modeling vortices, air ingestion, and swirl. The research compared full scale test results of a depressed horizontal outlet sump to results from two models, with scale ratios of 1:2 and 1:4 (24). No scale effects were detected for free surface vortex strength and persistence and consequent air ingestion over ranges of pipe Reynolds numbers from 7×10^4 to 9.3×10^5 and ranges of radial Reynolds number from 1.5 s 10^4 to 2.9×10^5. Using Froude scale velocity, the minimum model pipe Reynolds number is about 9.4×10^4 and the model radial Reynolds number is greater than 3×10^4. Therefore, no scale effects would be expected for vortex formation and swirl.

In conclusion, it has been demonstrated that the model scale ratio satisfies similitude requirements from several sources (4, 23, 24) and, therefore, no

scale effects would occur for the formation of vortices and swirl. Further, prototype velocity tests will be conducted to assure conservative results.

Dynamic Similarity of Flow Through Screens

In addition to providing protection from debris, screens tend to suppress non-uniformities of the approach flow. The aspects of flow through screens of concern in a model study are: (1) energy loss of fluid passing through the screen; (2) modification of velocity profile and deflection of streamlines at the screen; and (3) production of turbulence. As all these factors could affect vortex formation in a sump with approach flow directed through screens, a proper modeling of screen parameters is important.

The loss of energy across the screen occurs at a rate proportional to the loss in pressure, and this loss dictates the effectiveness of the screen in altering velocity profiles. The pressure drop across the screen is analogous to the drag induced by a row of cylinders in a flow field and could be expressed in terms of a pressure-loss coefficient K (or alternately a drag coefficient), defined as (8):

$$K = \frac{\Delta p}{1/2\ \rho\ U^2} = \frac{\Delta H}{U^2/2g} \qquad (11)$$

where

Δp = loss in pressure across the screen
U = mean velocity of approach flow
ρ = density of the fluid
ΔH = head across the screen
g = acceleration due to gravity

From the available literature on the topic (7, 8, 9), it may be seen that

$$K = f\ (R_s,\ S',\ \text{Pattern}) \qquad (12)$$

where

R_s = screen Reynolds number, $U\ d_w/\nu$, d_w being the wire diameter of the screen

S' = solidity ratio, equal to the ratio of closed area to total area of screen

Pattern = geometry of the wire screen

If the solidity ratio and the wire mesh pattern are the same in the model and prototype screens, the corresponding values of K would only be a function of the screen Reynolds numbers. This is analogous to the coefficient of drag in the case of the circular cylinder. It is known that K becomes practically independent of R_s at values of R_s greater than about 1000 (7, 10, 16). However, for models with low approach flow velocity and with fine wire screens, it is necessary to ascertain the influence of R_s on K for both the model and prototype screens before selecting screens for the model which are to scale pressure loss across the screens.

Velocity modification equations relating the upstream velocity profile and downstream velocity profile have been derived based on different theories (7). Most of these indicate a linear relationship between upstream velocity profile, and downstream velocity profile, shape and solidity ratio of screen, and value of K. If the wire pattern and solidity ratios are the same in the model and prototype screens, it is possible to select a suitable wire diameter to keep the values of K approximately the same for the model and prototype screens at the corresponding Reynolds number ranges. Identical velocity modification would be produced by the respective screens if the loss coefficients were identical.

The variation of pressure loss coefficients with Reynolds number for fine screens have been investigated at ARL (16). Based on the similarity of pressure loss and velocity modifications, model screens having the same percent open areas but mesh sizes and wire diameters approximately twice those of the prototype were chosen. Even with the larger mesh sizes, the model screens produce a conservative estimate of the head loss. The increased loss would produce somewhat greater velocity profile modification, however, screen blockages cause changes in velocity distributions far outweighing changes due to the screen alone.

MODEL DESCRIPTION

The model was constructed to a geometric scale of 1:2.98 with boundaries as indicated in Figure 1. Model boundaries were chosen at locations where flow pattern control in the prototype would be sufficiently removed from the sumps to minimize boundary effects, especially once screen blockage is considered. Screen blockage has consistently generated the most severe vortices and swirl in the numerous past containment recirculation sump studies at ARL (11, 13, 14, 25). The model was constructed as an elevated tank to provide sufficient room to install the sumps and to allow access to observe flow patterns in the sumps. Figure 6 shows the center section of the completed model. Figure 7 is a detail of the south sump showing the model grates and some appurtenant structures in the background. Figure 8 is a view of a sump from above showing the CS and RHR pump suction inlets. Figure 9 is a schematic of the model showing the modeled inlet piping and locations of flowmeters, pump, swirl meters, and piezometer taps. All suction lines were connected to a single pump by a manifold, so that any pump operation combination could be simulated.

A centrifugal pump recirculated water from the sumps back into the model at the boundary. Water level in the model was controlled by addition of water from a separate tank. Flow straighteners and screens at the model boundaries provided a uniform initial velocity distribution with relatively low turbulence levels. Portions of the prototype structure with outside dimensions greater than three inches, such as pipes, columns, pipe supports, and instrument boxes, in the immediate vicinity of the sumps and below the water surface, as shown in Figure 10, were modeled to the geometric scale.

The model was constructed basically of steel and wood with clear plastic windows at the sumps to allow observation of flow patterns. The suction pipes were modeled for about 35 pipe diameters. Since swirl and pressure loss measurements cannot be made simultaneously and the screen blockages were the same for both sumps resulting in similar losses and swirl, each sump was instrumented for one type of measurement. Suction pipes for the north RHR and CS pumps had swirl meters installed and suction pipes for the south RHR

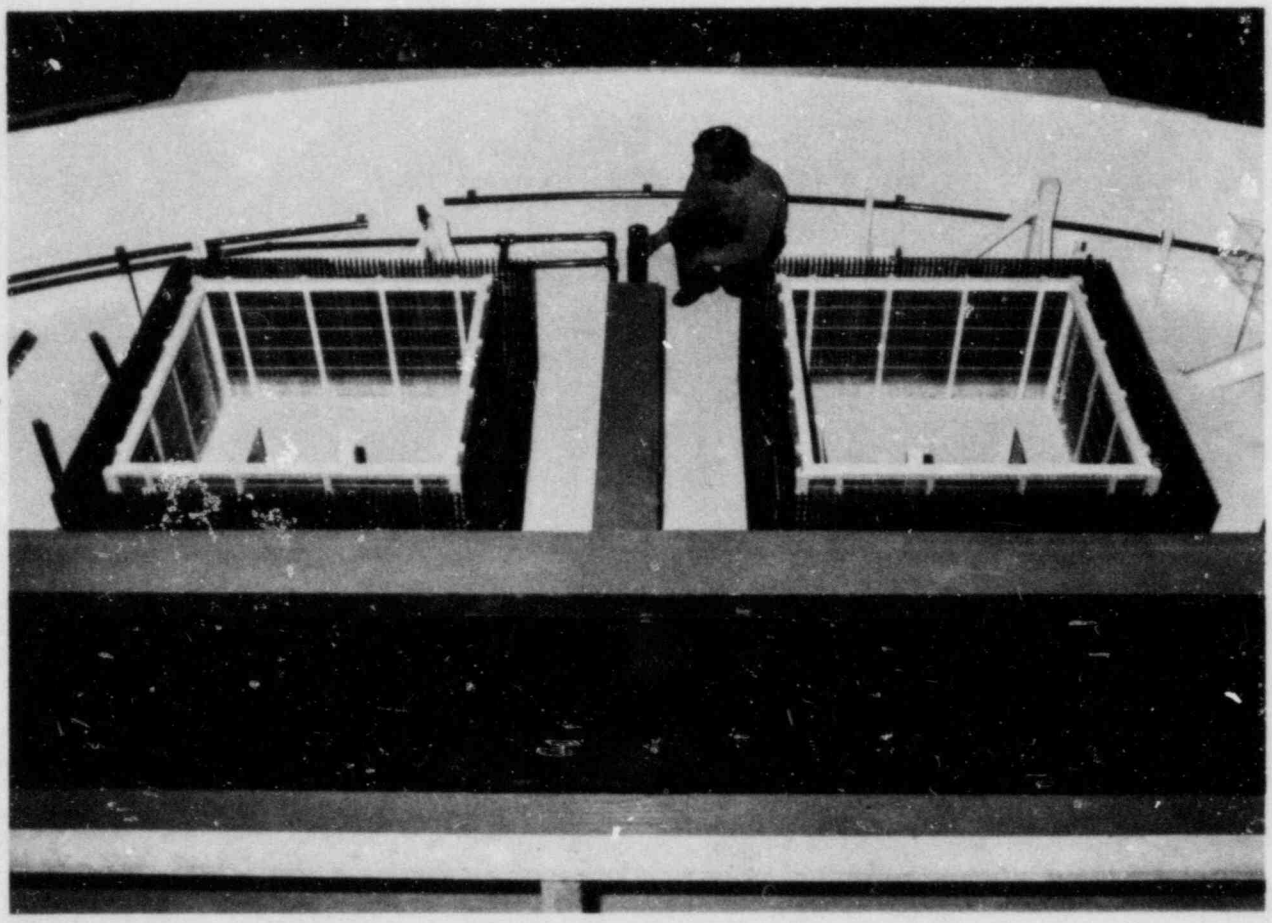

FIGURE 6 OVERALL VIEW OF MODEL

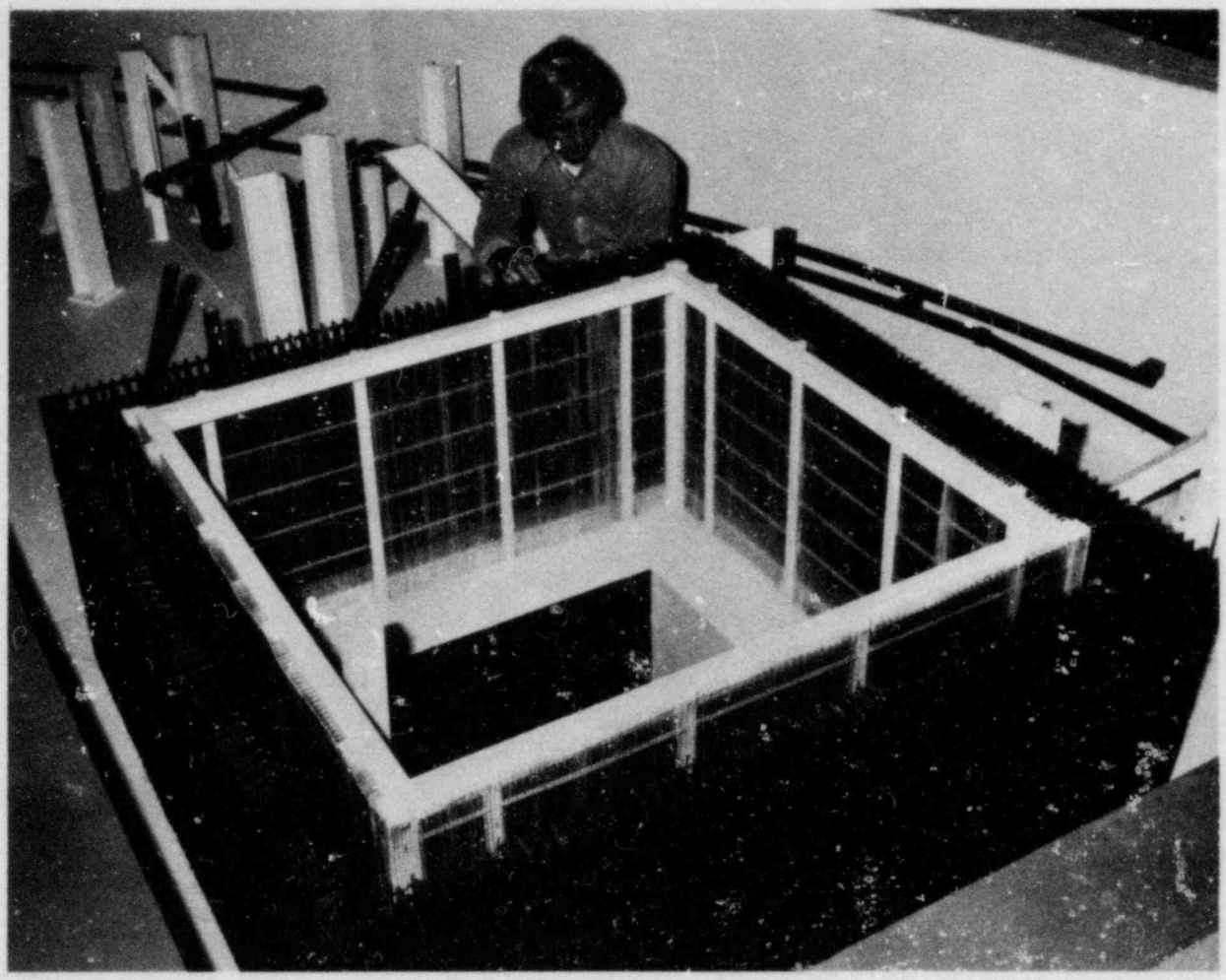

FIGURE 7 DETAILS OF SOUTH CONTAINMENT SUMP AND GRATINGS WITH SCREENS

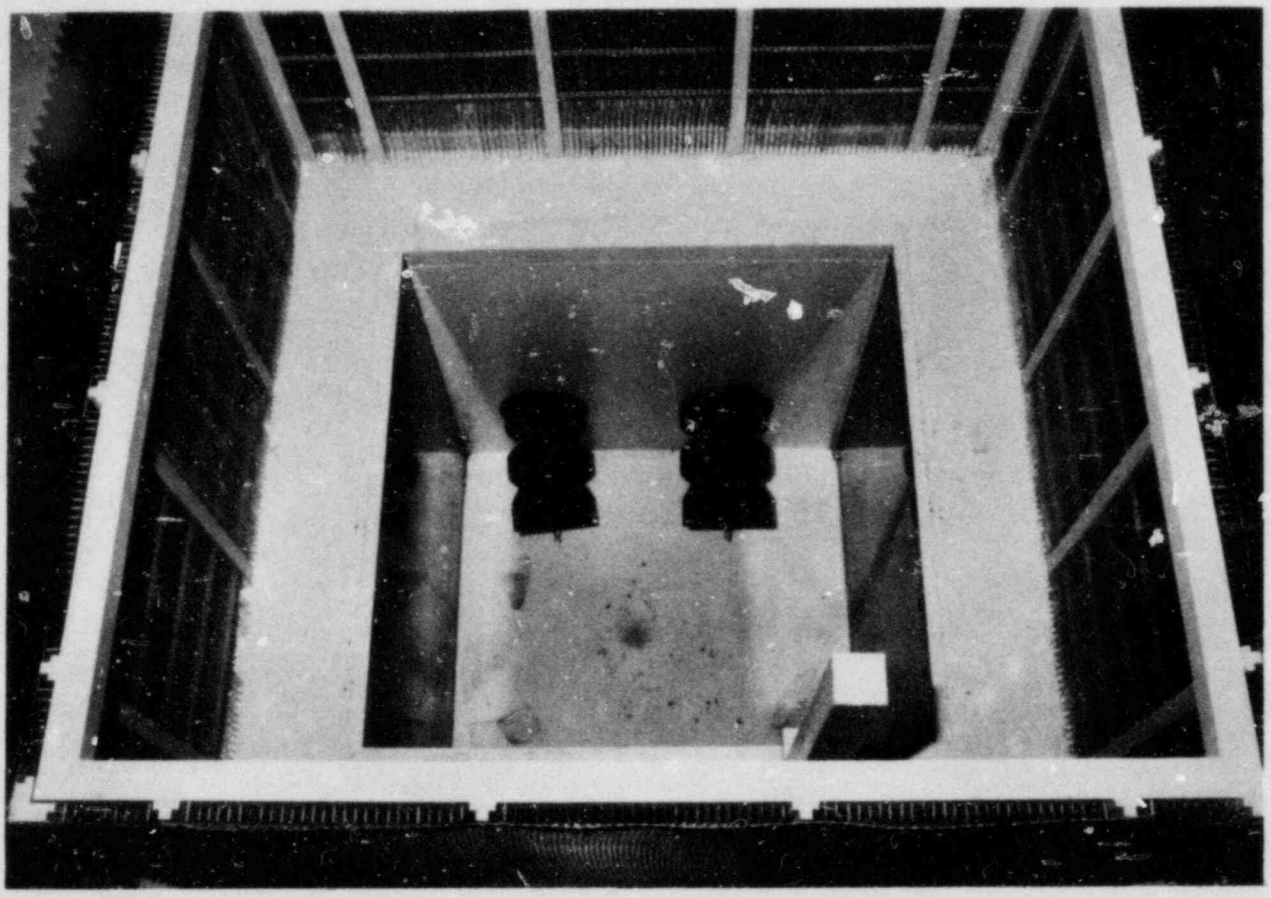

FIGURE 8 VIEW OF PUMP SUCTION LINES FROM ABOVE

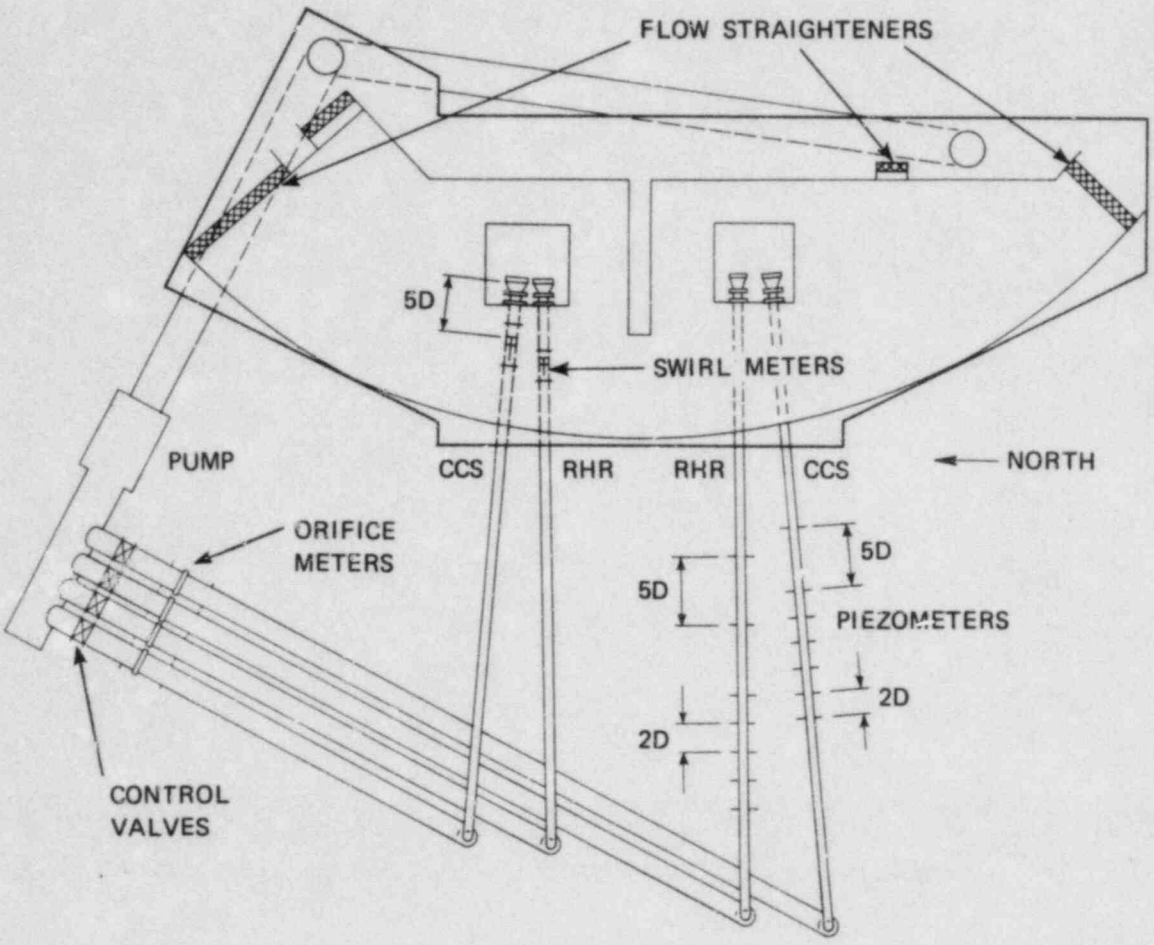

FIGURE 9 SCHEMATIC OF MODEL LAYOUT

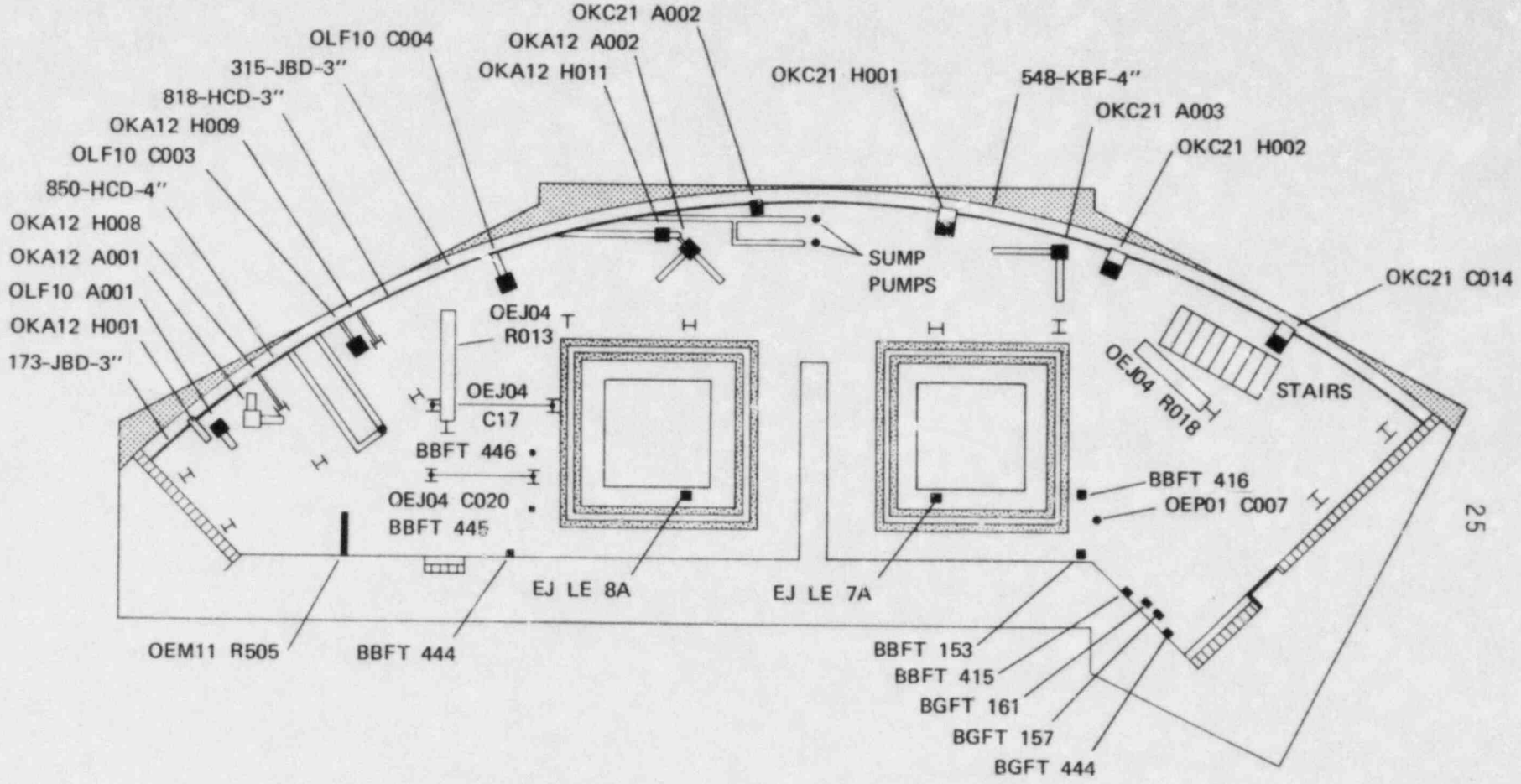

FIGURE 10 MODELED APPURTENANT STRUCTURES

and CS pumps had seven sets of piezometers for pressure gradeline measurement. Orifice flowmeters, constructed to ASME standards, were provided to measure flow in each suction line.

To increase model screen Reynolds numbers and thereby achieve model screen head losses simulating prototype head losses, model screens had larger mesh sizes than the prototype screens. The coarse screen was one inch mesh with 0.120 inch wire diameter, and the fine screen was 1/4 inch mesh with 0.032 inch wire diameter. In comparison, the prototype has a coarse screen with 1/2 inch mesh 0.063 inch wire diameter and fine screen with seven mesh with 0.018 inch wire.

The pump suction lines were modeled using four inch schedule 40 (4.026 inch ID) PVC pipe and 4.5 inch ID seamless steel tube which closely approximated the inside diameters of the CS and RHR suction lines, respectively.

The three prototype bar racks could not be modeled individually with commercially available floor grating. To assure correct flow patterns in the sump, the innermost grating was specially fabricated with the correct bearing bar depth, width, and spacing. Since the innermost grating controlled the flow patterns, the outer two gratings were approximated by a single standard 1½ inch floor grating. The model outer grating simulated the total depth of the two prototype grates and had a ratio of bearing bar depth to spacing equal to a single grate. Therefore, the model would produce somewhat less effective flow straightening than the prototype and is, therefore, conservative.

INSTRUMENTATION AND OBSERVATION TECHNIQUES

Flow Measurement

Flowrates were measured by orifice meters constructed to ASME standards and coefficients calculated by ASME methods (20) using air-water manometers for differential pressure measurement. The orifice meters in the CS pump suction lines had diameters of 3.787 and 3.788 and the RHR pump suction lines had orifice diameters of 4.251 inches. Sensitivity analyses showed that the average diameter for each pair of orifices could be used without adversely affecting measurement accuracy (maximum error introduced is less than 0.1 percent). Likewise, an average discharge coefficient was used based on the Reynolds number at water temperature 60°F and the average flowrate for each orifice size. A flow measurement uncertainty of ±2 percent is predicted using ASME estimates for uncertainty of discharge coefficient and ASME uncertainty estimation procedures (20).

Vortex activity and suction pipe inlet swirl have been shown to be essentially independent of Reynolds number and weak functions of Froude number (24). Small changes in flowrate have no effect on vortex strength and swirl and a flow measurement accuracy of 2 percent is adequate. Therefore, physical calibration of the flowmeters was not required.

Pressure Gradelines

The pressure gradelines in the south RHR and CS suction lines were measured by pairs of piezometers at seven locations as shown in Figure 9 using air-water manometers with the sump water level as reference pressure. The pressure gradeline was extrapolated to the pipe entrance by a linear least squares curve fit of the pressure measurements. The area average velocity was used to calculate the pipe velocity head, which was added to the extrapolated pressure gradeline. The pipe total head was subtracted from the sump total head to

determine the inlet loss. An entrance loss coefficient, including the loss due to the screens, was calculated by:

$$K = \frac{\Delta H_i}{\frac{U^2}{2g}} \qquad (13)$$

where

K = loss coefficient

ΔH_i = inlet head loss, ft

Pipe Swirl

Average swirl in the suction pipes was measured by a cross-vane swirl meter located two pipe diameters downstream of the inlet. Studies at ARL (17) have shown that a swirl meter with vane diameter 80 percent of the pipe diameter best approximates the solid body rotation of the flow. The rate of rotation of the swirl meter was determined by counting the number of vanes passing a fixed point in two minutes.

An average swirl angle was defined as the arc tangent of the maximum tangential velocity divided by the mean axial velocity. The maximum tangential velocity is the rotational speed (N) times the circumference of the pipe, π d. The average swirl angle is defined by:

$$\theta = \text{arc tan } (\frac{\pi \ d \ N}{U}) \qquad (14)$$

where

N = revolutions per second
d = pipe diameter, ft
U = mean axial velocity, ft/sec

Vortex Activity

Vortex activity was recorded by observing vortex strength on a scale from 1 to 6 (see Figure 11). Vortex strength was identified by using dye injection or addition of "trash" consisting of a sightly buoyant ball of paper when required.

Observation of Flow Patterns

Visual aids, such as dye, were used to observe flow patterns. Photographic documentation was taken whenever appropriate.

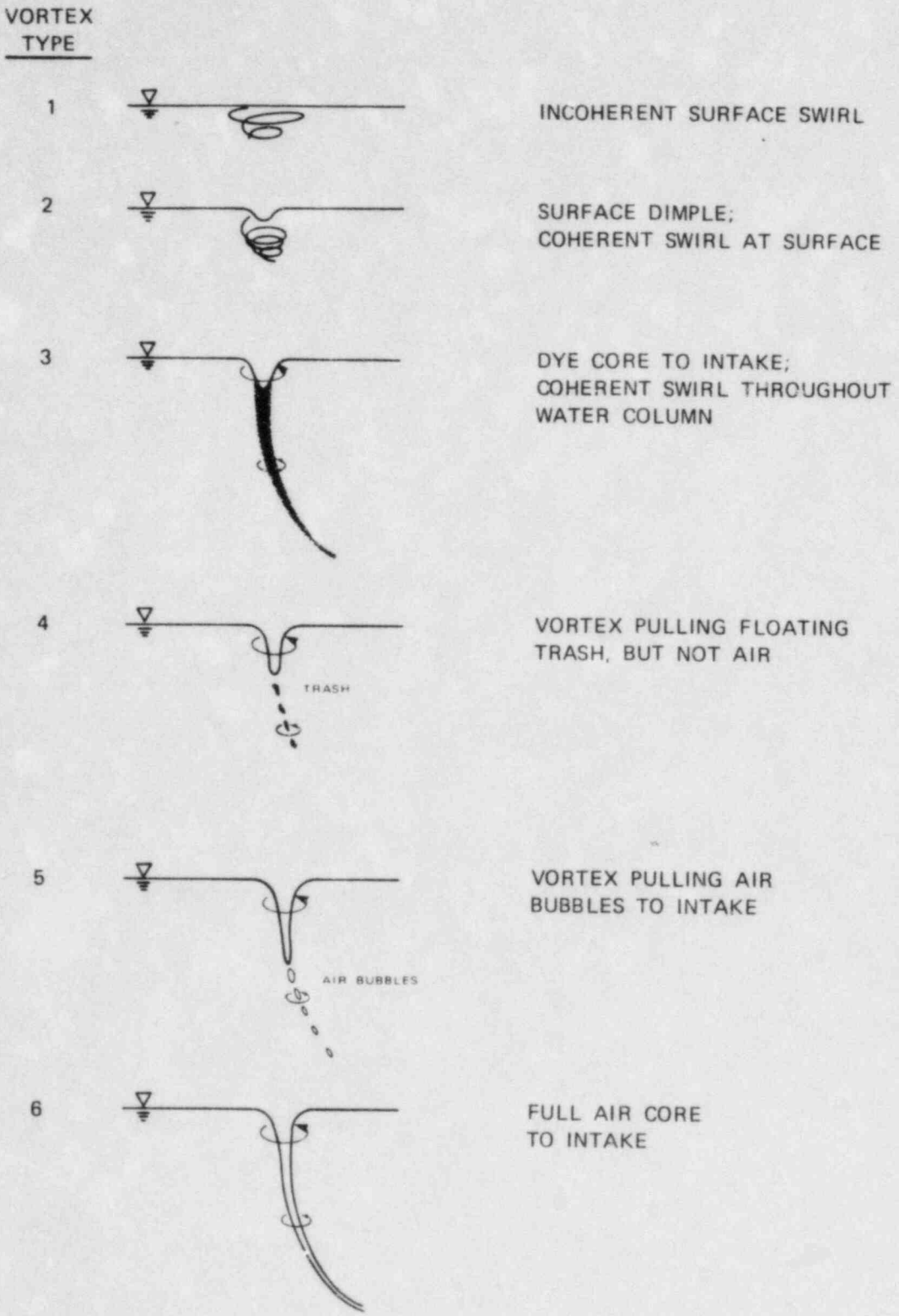

FIGURE 11 CLASSIFICATION OF FREE SURFACE VORTICES

TEST PROCEDURE

Tests were conducted at the normal laboratory water temperature, approximately 60°F. The model was filled to an appropriate level, and all piezometer and manometer lines were purged of air and zero flow differentials checked. The required flowrates were then set and allowed to stabilize. The water level was checked, adjustments made if required, and flowrates were rechecked and readjusted, if necessary. A 15 minute minimum settling time was allowed prior to initiation of the data recording. Fifteen minutes of vortex observations were recorded and the required physical parameters, such as depth, manometer deflections, and swirl meter readings, were recorded.

TEST RESULTS

Since the location of the postulated pipe break within the containment is not predictable, the effect of boundary conditions on the sump performance must be determined. Therefore, five boundary conditions were used to determine sensitivity of hydraulic performance. The boundary conditions were based on the four flow distributors located at the model boundaries. Four boundary conditions, achieved by blocking the flow distributors, are shown in Figure 12. The fifth boundary condition distributed flow based on the distribution area without blockage. The four boundary conditions with blocked distributors represent extreme boundary conditions.

Original Design Performance

The evaluation of the original design was conducted with the five boundary conditions with four-pump and two-pump operation. Both Froude scale velocity and prototype velocity were used to demonstrate the effect of the velocity scale.

Table 2 lists the maximum strength vortex noted during the test without regard to persistence. For two-pump operation at prototype velocity, an air core vortex (type 6) occurred for boundary condition A and a vortex pulling air bubbles (type 5) occurred for boundary condition D. Froude scale velocity resulted in type 4 vortices (trash pulling vortices) for boundary conditions A and D. Four-pump operation at water level 2003 ft 6 1/2 inches resulted in type 4 vortices for both Froude and prototype scale velocity. Boundary condition A and D were determined to result in the most severe vortex action and were chosen to be used in the remainder of the test program in conjunction with the unblocked flow distributor case, which would be the more likely boundary condition in the prototype.

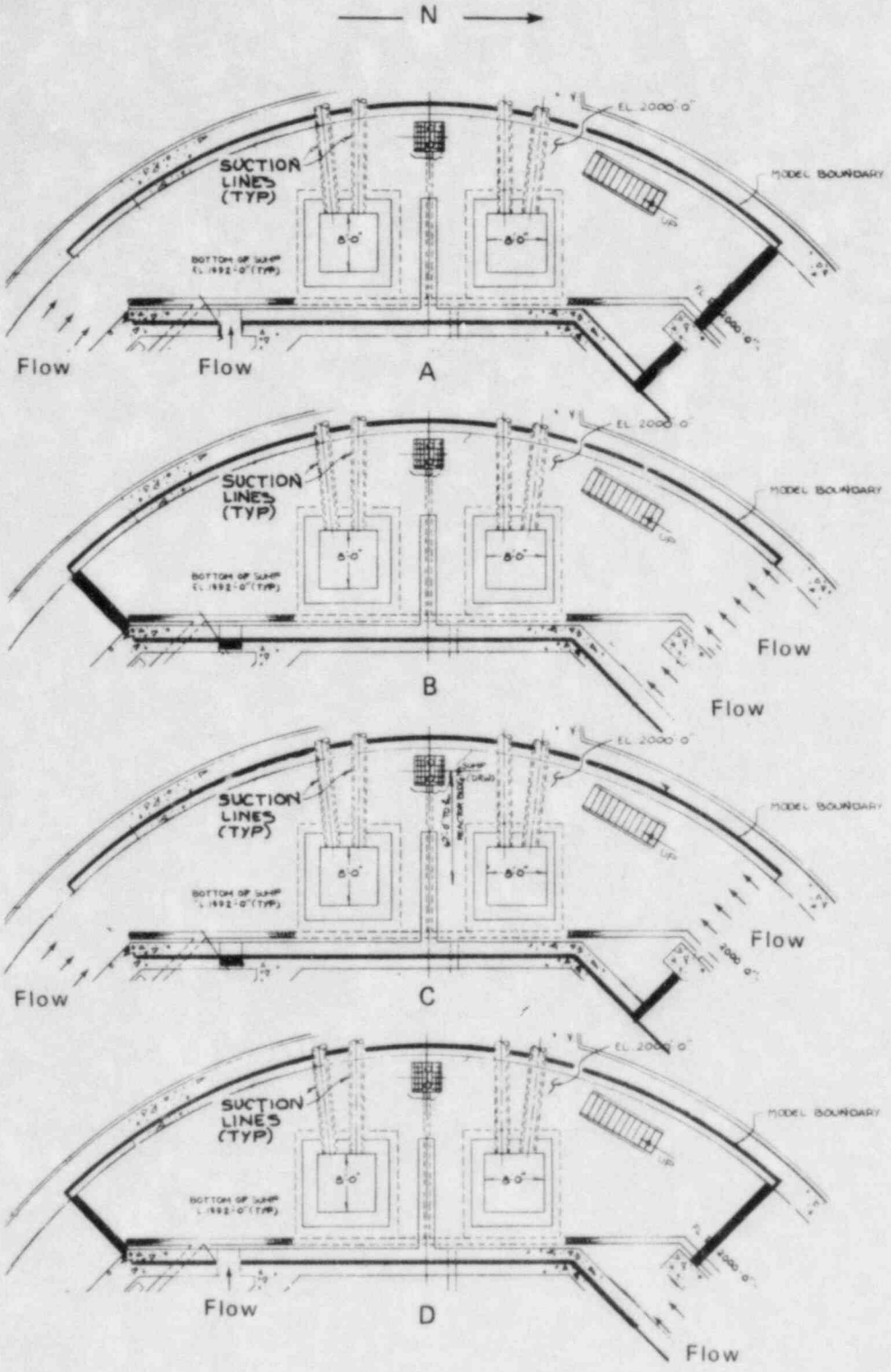

FIGURE 12 FLOW BOUNDARY CONDITIONS

TABLE 2

MAXIMUM VORTEX STRENGTH

Boundary Condition Sensitivity Tests

Boundary Condition[1]	Four Pumps		Two Pumps	
	F	P	F	P
0	3	4	1	2
A	2	4	4	6
B	2	3	3	4
C	2	2	1	2
D	4	4	4	5

NOTES: F - Froude Scale Velocity
P - Prototype Velocity
1 - See Figure 12
See Figure 11 for definition of vortex strength

Table 3 lists the maximum vortex strength for Froude scale velocity and boundary condition 0 (no flow distributor blockage) with the eight screen blockage configurations shown in Figure 13. Air core vortices were noted in three cases and two other cases had vortex strengths greater than a type 3 (dye core). Figure 14 shows the air core vortex formed with screen blockage 1.

TABLE 3

MAXIMUM VORTEX STRENGTH

Screen Blockage Tests

Screen Blockage	Vortex Strength
1	6
2	6
3	2
4	2
5	4
6	1
7	5
8	6

NOTES: Four-pump operation at Froude scale velocity
Boundary Condition 0

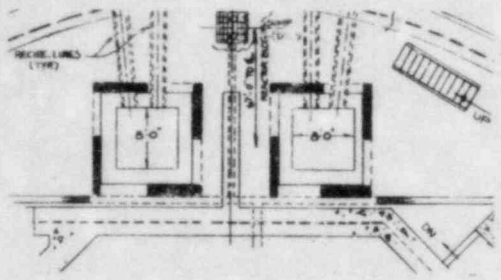

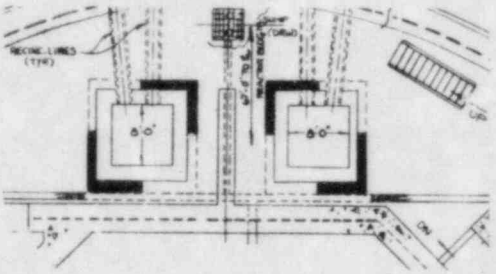

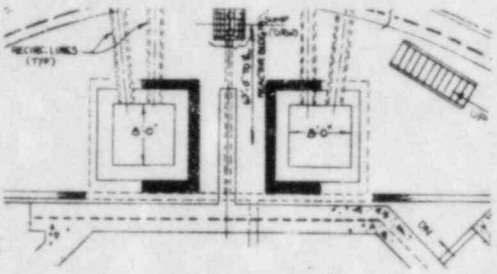

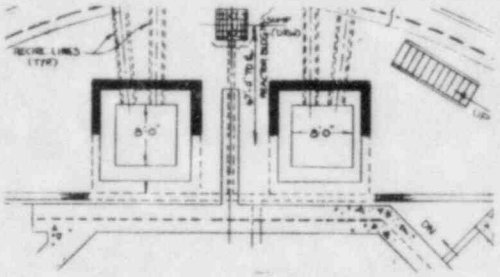

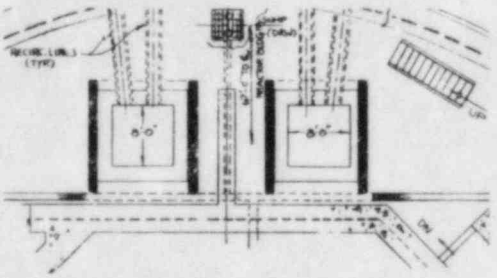

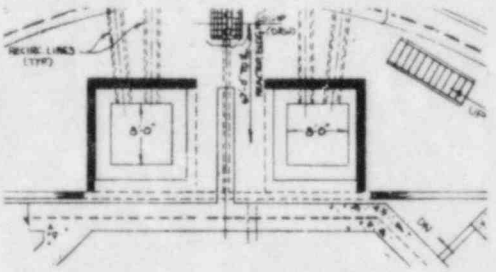

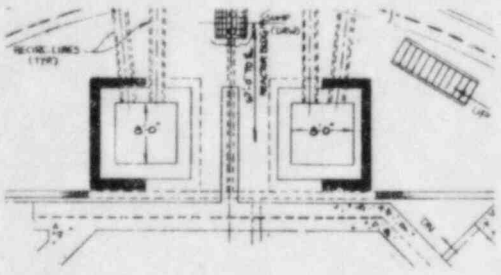

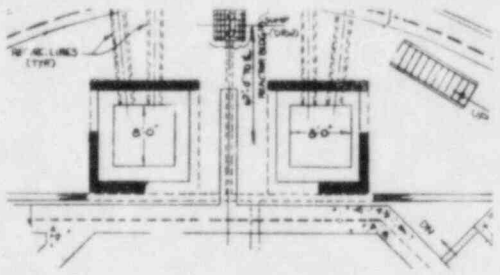

FIGURE 13 SCREEN BLOCKAGE GEOMETRIES

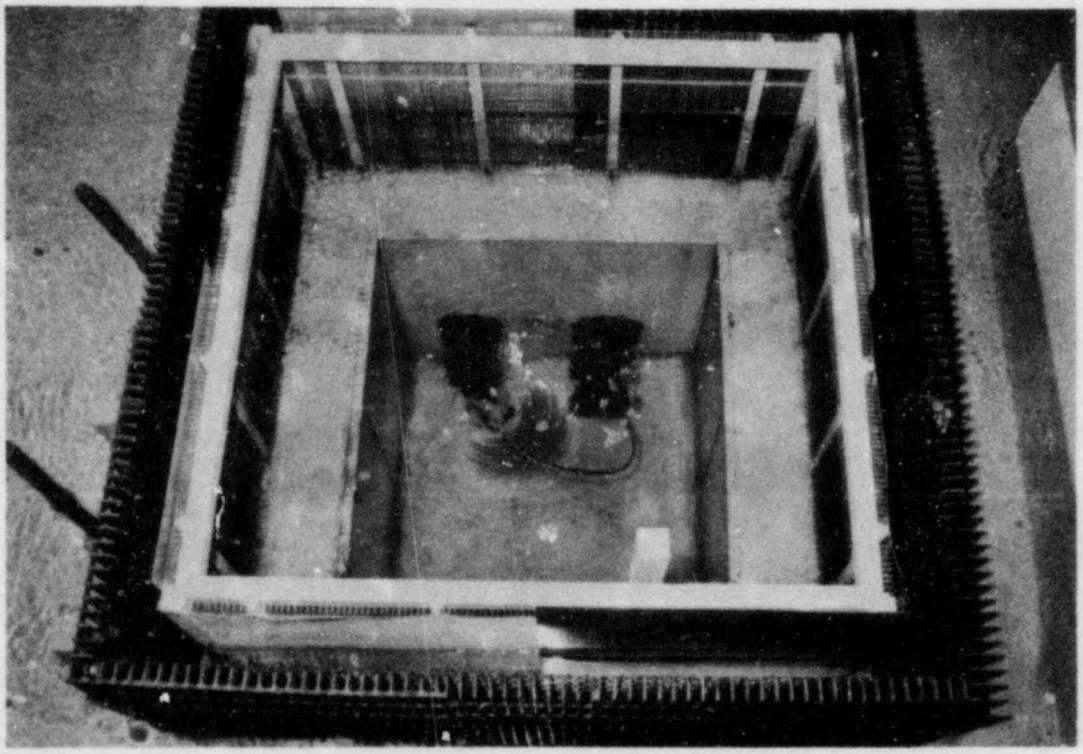

FIGURE 14 AIR-CORE VORTEX FORMED BY SCREEN BLOCKAGE 1

Since the maximum vortex strength occurring was greater than the design criterion (a type 3 dye core vortex) a vortex suppression device was deemed necessary.

Swirl angles measured during the boundary condition sensitivity tests are listed in Table 4. Maximum swirl angles measured were 2.0 and 1.0 degrees for the RHR and CS suction lines, respectively. The average values were 1.0 and 0.6 degrees, respectively. In most cases the agreement between the Froude scale velocity and prototype velocity was within about 0.2 degrees. Table 5 lists swirl angles for the eight screen blockages. The maximum swirl angles were 1.5 and -1.0 for the RHR and the CS suction lines, respectively. Average swirl angles were 0.8 and 0.4, slightly less than in the boundary condition sensitivity tests. It will be noted that swirl angle does not correlate with vortex type.

TABLE 4

SWIRL ANGLE

Boundary Condition Sensitivity Tests

Boundary Condition[1]	Four Pump				Two Pump	
	CS		RHR		RHR	
	F	P	F	P	F	P
0	-0.9	-0.3	-1.4	-0.9	-0.9	-1.0
A	-0.6	-0.3	-0.2	-0.1	-0.4	-0.6
B	-1.0	-0.5	-0.9	-1.1	-1.9	-2.0
C	-0.7	-0.8	-1.4	-1.6	-0.7	-0.9
D	-0.3	-0.5	-0.6	-0.9	-1.3	-1.4

NOTES: F - Froude Scale Velocity
P - Prototype Velocity
1 - See Figure 12
Angles in Degrees
Negative is counterclockwise looking downstream

TABLE 5

SWIRL ANGLE

Screen Blockage Tests

Screen Blockage[1]	Swirl Angle	
	CS	RHR
1	0.1	0.3
2	-1.0	-1.1
3	-0.7	-0.8
4	-0.5	-0.5
5	-0.2	-0.4
6	0.3	1.5
7	-0.1	0.6
8	-0.5	-1.2

NOTES: Froude Scale Velocity
Four-pump operation
Boundary Condition 0
1 - See Figure 13

Vortex Suppressor Test Results

Experience (25, 27) has shown standard floor grating to be an effective vortex suppressor when the grating is close enough to the water surface. The same grating as used for the screen system (2 inch x 3/16 inch on 19/16 inch centers) was chosen for the vortex suppressor. The grating was placed at the containment floor level (2000 ft 0 inches) over the entire sump. The bearing bars were oriented in the direction of the containment radius. Figure 15 shows the grating in place and a cross-section detail of the grating.

A series of Froude scale velocity tests were conducted with all eight screen blockage geometries for both two-pump and four-pump operation. The three boundary conditions O, A, and D, resulting in the more severe vortex activity were chosen to be tested with the screen blockages. About one-half of the tests - those with screen blockages, 2, 4, 6, 8, and clean screens - were then conducted with prototype velocity.

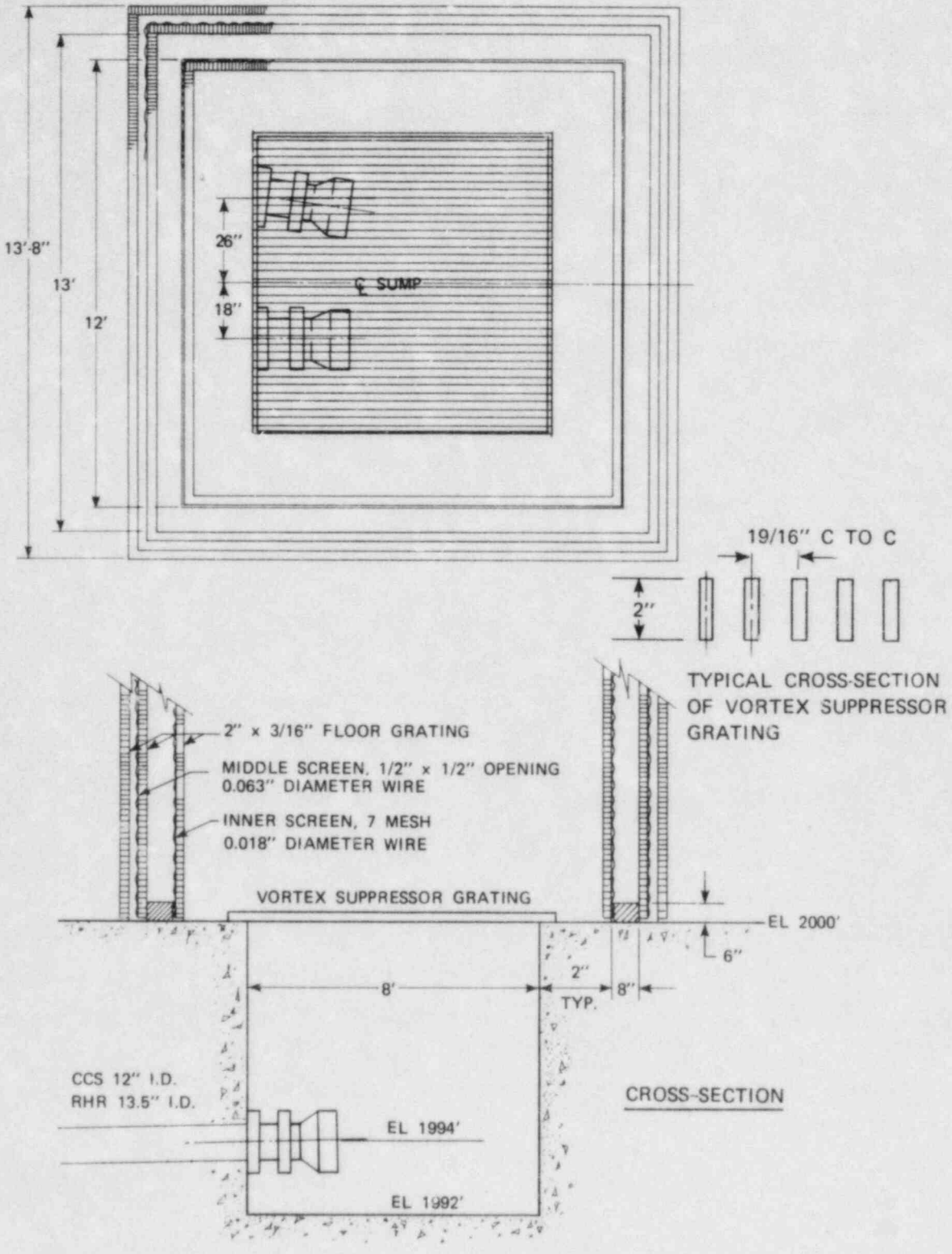

FIGURE 15 PLACEMENT AND CROSS-SECTION OF VORTEX SUPPRESSOR GRATING OVER CONTAINMENT RECIRCULATION SUMP

Table 6 lists the maximum vortex strength noted. A type 2 vortex was the greatest vortex strength noted, indicating the suppressor design was adequate.

Figure 16 shows the performance of the sump with the vortex suppressor in place with screen blockage 1 and may be compared to Figure 14 which was the same condition without the vortex suppressor.

Table 7 lists the swirl angles measured for the CS and RHR suction lines. The maximum swirl angles determined were -1.6 and -1.4 degrees for the CS and the RHR lines occurring for boundary condition A and screen blockage seven. Average swirl angles, determined without regard to direction of rotation, were 0.4 and 0.6 degrees for the CS and the RHR lines for four-pump operation and 0.4 for the RHR line for two-pump operation. These values are lower than the average values for the boundary sensitivity tests without the vortex suppressor. Since the suppressor is mounted at floor level, below the screens inducing vorticity, the suppressor is effective in decreasing both vortex activity and swirl. The measured swirl angles are quite small, due to the effective swirl suppressor design at the inlet and are of no practical significance since a single bend in the suction line would produce significantly greater swirl.

Since the RHR pumps would operate alone in the recirculation mode until CS pump realignment at water level 2003 ft 6-1/2 inches, testing included RHR pump operation at the initial water level of 2002 ft 4 inches as well as at two higher water levels (2002 ft 11 inches and 2003 ft 6-1/2 inches) to assure no adverse conditions would occur. Four screen blockages were used with boundary condition 0. Table 8 summarizes the test results for the three water levels tested. No significant vortex action was seen for any cases. Swirl angle was essentially the same in all cases and the values were not of practical significance.

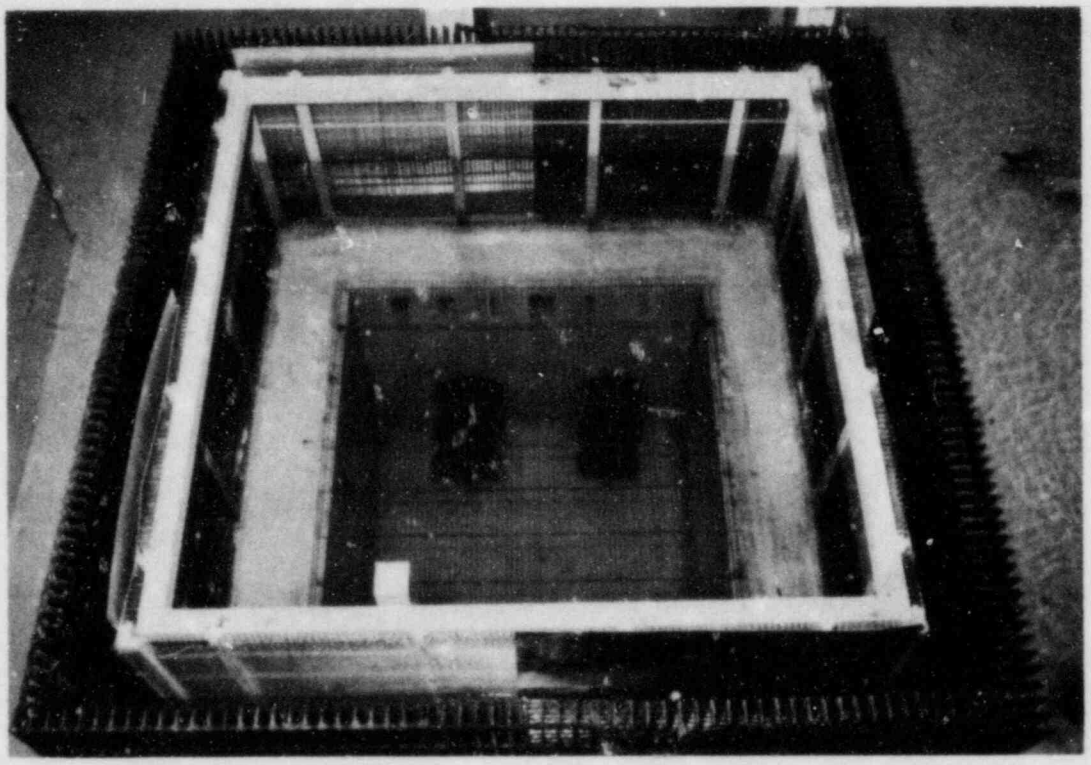

FIGURE 16 SUMP PERFORMANCE WITH VORTEX SUPPRESSOR, SCREEN BLOCKAGE 1

TABLE 6

MAXIMUM VORTEX STRENGTH WITH VORTEX SUPPRESSOR
(see Figure 11)

		Four-Pump Operation		Two-Pump Operation	
Boundary Condition[1]	Screen Blockage[2]	Froude Velocity	Prototype Velocity	Froude Velocity	Prototype Velocity
C	0	1	2	1	1
0	1	1		1	
0	2	1	2	1	1
0	3	1		1	
0	4	2	2	1	2
0	5	2		1	
0	6	1	2	1	2
0	7	1		1	
0	8	1	2	1	2
A	0	1	2	1	1
A	1	2		1	
A	2	1	2	1	2
A	3	1		1	
A	4	2	2	1	2
A	5	1		1	
A	6	1	2	1	2
A	7	1		1	
A	8	2	2	1	2
D	0	1	2	1	2
D	1	2		1	
D	2	1	2	1	2
D	3	1		1	
D	4	2	2	1	2
D	5	2		1	
D	6	1	1	1	1
D	7	1		1	
D	8	2	2	1	2

NOTES: 1 - See Figure 12

2 - See Figure 13

TABLE 7

SWIRL ANGLE WITH VORTEX SUPPRESSOR

		Four-Pump Operation				Two-Pump Operation	
		CS		RHR		RHR	
Boundary Condition[1]	Screen Blockage[2]	Froude	Prototype	Froude	Prototype	Froude	Prototype
0	0	0.2	0.3	-0.7	-0.8	-0.1	0.1
0	1	-0.2		0.1		0.4	
0	2	-0.8	0.1	-0.9	-0.3	0.2	0.7
0	3	0.3		-0.8		0.7	
0	4	-0.2	-0.6	-1.1	-1.1	0.4	0.6
0	5	-0.6		-0.8		-0.1	
0	6	-0.7	0.3	-0.2	-0.3	-0.2	-0.1
0	7	-0.1		-0.1		-0.3	
0	8	0.6	0.8	-0.9	-0.7	0.1	0.1
A	0	0.2	0.1	0.1	-0.1	0.0	0.1
A	1	0.6		0.7		0.8	
A	2	0.1	0.2	0.4	0.3	-0.3	-0.1
A	3	-0.3		0.2		0.6	
A	4	-0.5	-0.7	-0.6	-0.8	0.4	-0.2
A	5	0.1		-0.5		0.3	
A	6	-0.4	-0.1	-0.6	-0.8	-0.2	-0.8
A	7	-1.6		-1.4		-0.4	
A	8	-0.9	0.3	-0.4	-0.2	-0.1	-0.2
D	0	-0.1	-0.1	-0.7	-0.3	-0.1	0.1
D	1	0.5		0.2		0.4	
D	2	-0.8	-0.1	-1.0	-0.4	-0.3	-0.7
D	3	0.1		0.2		1.0	
D	4	-0.9	-0.7	-0.1	-1.2	0.1	0.2
D	5	-0.3		-0.2		-0.4	
D	6	0.6	0.3	-1.2	-0.7	0.1	-0.5
D	7	0.3		-0.3		0.1	
D	8	-0.6	-0.3	-1.1	-0.6	0.1	-0.6

NOTES: 1 - See Figure 12

2 - See Figure 13

Negative is counterclockwise looking downstream

TABLE 8

TWO-PUMP OPERATION, VARYING WATER LEVEL

Water Level	Maximum Vortex Strength			Swirl Angle		
	2000'4"	2002'11"	2003'6-1/2"	2002'4"	2002'11"	2003'6-1/2"
Screen Blockage[1]						
2	1	1	1	0.2	0.4	0.1
4	1	1	1	0.4	0.5	-0.1
6	1	1	1	-0.2	-0.4	0.3
8	1	1	1	0.1	-0.3	-0.3

NOTE: Froude Scale Velocity Boundary Condition 0

1 - See Figure 12

Inlet Loss Coefficient

The pressure gradelines in the RHR and CS suction lines were measured during all Froude scale velocity tests. An inlet loss coefficient was calculated for each suction line by Equation (13). The loss coefficient included the cumulative losses through the gratings, screens with 50 percent blockage, inlets, and vortex breakers. The data indicated a loss coefficient for the CS suction line of 0.35 and an RHR suction line inlet loss coefficient of 0.25. Considering the geometric similarity of the two inlets, the variation in the inlet coefficients between the RHR and CS suction line inlets was unexpected and further tests were conducted to determine the source of the difference. Since any error in flow measurement translates into a relatively large error in determination of the loss coefficient, the flow meters were removed and calibrated by the gravimetric method. Calibration data indicated a variation of 0.5 percent and 0.8 percent in the discharge coefficients from those predicted by the ASME Fluid Meters Handbook. These variations were insufficient to account for the differences in loss coefficient. To increase the accuracy of the pressure gradeline measurement, a point gauge with 0.001 ft graduations was used to measure the pressure gradeline instead of a ruler with 0.01 ft graduations. Figure 17 shows the results from the CS suction line inlet indicating essentially no change in the average loss coefficient, 0.35, from the previous data. However, Figure 18 shows that the RHR data has a loss coefficient of 0.32. This result agrees much better with the CS suction line inlet coefficient, as was expected from the geometrical similarity.

For design purposes, the larger coefficient of 0.35 should be used for both suction line inlets. In terms of actual head loss, a difference of 0.03 in loss coefficient corresponds to a variation in head of 0.06 ft so that the uncertainty in the total head is small and not of practical significance. The measured inlet loss coefficient was less than that calculated by Bechtel, 0.46, (30) and, therefore, additional net positive suction head is available to the RHR and CS pumps than was considered in the plant design.

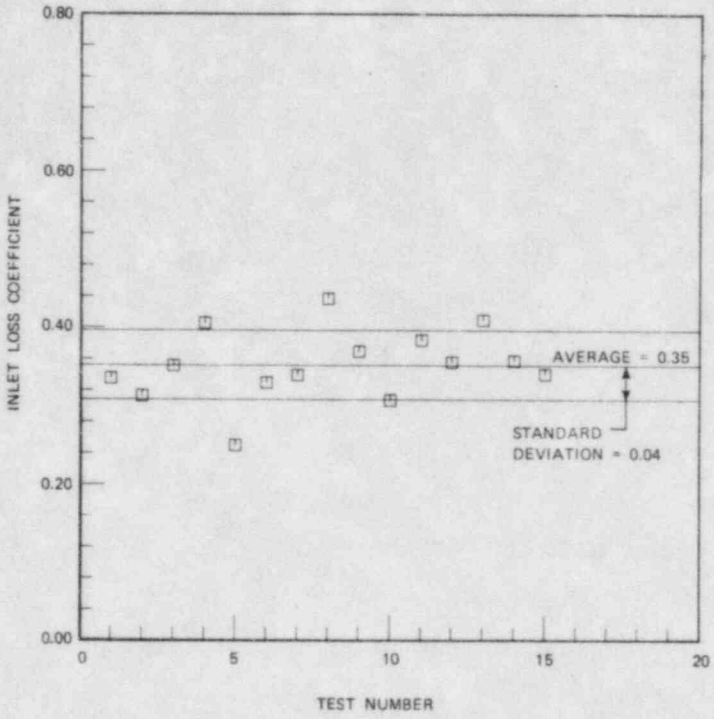

FIGURE 17 INLET LOSS COEFFICIENT, CS SUCTION LINE

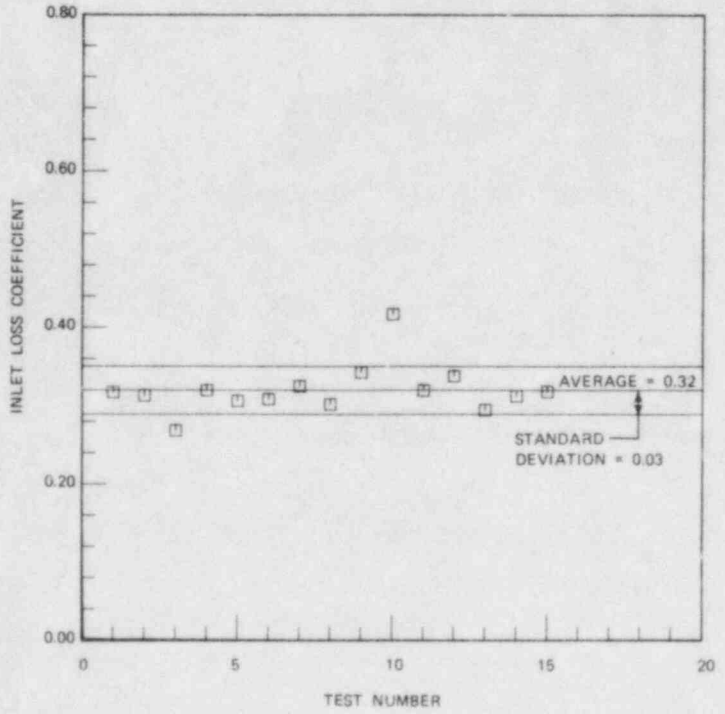

FIGURE 18 INLET LOSS COEFFICIENT, RHR SUCTION LINE

SUMMARY

A 1:2.98 scale model of the containment recirculation sumps for the Standardized Nuclear Unit Power Plant System was constructed and tested. A variety of possible boundary conditions, bar rack and screen blockages, and water levels and pump operation combinations were tested to simulate possible undesirable flow patterns which could result in poor pump performance during the recirculation mode. The model was operated with both Froude scale velocity and prototype velocity. Vortex activity was observed and the maximum strength vortex was recorded. The flow rotation in the suction pipes and head losses due to the bar rack, screens, and inlet geometry were also measured.

Initial tests indicated that an air core vortex was likely to form, especially with screen blockage. It was determined that a vortex suppressor was required. The chosen vortex suppressor consisted of floor grating covering the entire sump at containment floor level, elevation 2000 ft 0 inches. In about 100 tests with this vortex suppressor in place with varied water levels, boundary conditions, screen blockages, and pump combinations, the maximum strength vortex was a surface dimple (type 2), which is acceptable sump performance.

Solid body rotation of the flow in one CS and one RHR suction line was measured by a swirl meter. The maximum swirl angle determined was 1.6 degrees. Average swirl angle was about 0.4 degrees. The swirl angles measured were acceptable.

Inlet loss coefficients were determined in one CS and one RHR suction line. With 50 percent screen blockage, the inlet loss coefficient was about 0.35, which included the screen losses. This measured loss coefficient was less than that calculated by Bechtel and thus additional NPSH is available than was considered in design calculations.

REFERENCES

1. Daggett, L.K., and Keulegan, G.H., "Similitude Conditions in Free Surface Vortex Formations," Journal of Hydraulics Division, ASCE, Vol. 100, pp. 1565-1581, November 1974.

2. Daily, J.W., and Harleman, D.R.F., Fluid Dynamics, Addision-Wesley Publishing Company, 1965.

3. Rouse, H., Handbook of Hydraulics, John Wiley & Sons, 1950.

4. Anwar, H.O., Weller, J.A., and Amphlet, M.B., "Similarity of Free Vortex at Horizontal Intake," Journal of Hydraulic Research, IAHR 16, No. 2, 1978.

5. Hattersley, R.T., "Hydraulic Design of Pump Intakes," Journal of the Hydraulics Division, ASCE, pp. 233-249, March 1965.

6. Reddy, Y.R., and Pickford, J., "Vortex Suppression in Stilling Pond Overflow," Journal of Hydraulics Division, ASCE, pp. 1685-1697, November 1974.

7. Baines, W.D., and Peterson, E.G., "An Investigation of Flow Through Screens," Trans. ASME, pp. 467-477, July 1951.

8. Papworth, M., "The Effect of Screens on Flow Characteristics," British Hydromechanics Research Association, Report TN1198, November 1972.

9. Weighardt, K.E.G., "On the Resistance of Screens," The Aeronautical Quarterly, Vol. IV, February 1953.

10. Tennessee Valley Authority, "Flow Through Screens," Report No. 87-8, May 1976.

11. Padmanabhan, M., "Hydraulic Model Studies of the Reactor Containment Building Sump, North Anna Nuclear Power Station - Unit 1," ARL Report No. 123-77/M250CR, July 1977.

12. Durgin, W.W., and Hecker, G.E., "The Modeling of Vortices at Intake Structures," Joint Symposium of Design and Operation of Fluid Machinery, Colorado State University, June 1978.

13. Padmanabhan, M., "Hydraulic Model Investigation of Vortexing and Swirl Within a Reactor Containment Recirculation Sump," Donald C. Cook Nuclear Power Station, ARL Report No. 108-78/M178FF.

14. Padmanabhan, M., "Assessment of Flow Characteristics Within a Reactor Containment Recirculation Sump Using a Scale Model," McGuire Nuclear Power Station, ARL Report No. 29-78/M208JF.

15. Padmanabhan, M., "Selection and Scaling of Horizontal Gratings for Vortex Suppression," ARL Report No. 68-78, July 1978.

16. Padmanabhan, M., and Vigander, S., "Pressure Drop Due to Flow Through Fine Mesh Screens," Journal of the Hydraulics Division, ASCE, HY8, August 1978.

17. Durgin, W.W., and Lee, H.L., "The Performance of Cross-Vane Swirl Meters," ASME Winter Annual Meeting, 1980.

13. Miller, D.S., Internal Flow Systems, BHRA Fluid Engineering, 1978.

19. Padmanabhan, M., "Investigation of Vortexing and Swirl Within a Containment Recirculation Sump Using a Hydraulic Model," ARL Report No. 25-81/M296HF, February 1981.

20. Fluid Meters, The American Society of Mechanical Engineers, Sixth Edition, New York. New York, 1971.

21. Unpublished ARL Experimental Results.

22. Angelin, S., and Larsen, P., Discussion of "Factors Influencing Flow in Large Conduits," Journal of the Hydraulics Division, ASCE, July 1966.

23. Hecker, G.E., "Model-Prototype Comparison of Free Surface Vortices," Journal of the Hydraulics Division, ASCE, Vol. 107, No. HY10, October, 1981.

24. Padmanabhan, M. and Hecker, G.E., "Assessment of Scale Effects on Vortexing, Swirl, and Inlet Losses in Large Scale Sump Models," ARL Report No. 48-82/M398F.

25. Nystrom, J.B., "Experimental Evaluation of Flow Patterns in an RHR Sump with Simulation of Screen Blockage," ARL Report No. 24-81/M302LM.

26. Padmanabhan, M., "A Parametric Study of Containment Emergency Sump Performance," ARL Report No. 46A-82.

27. Padmanabhan, M., "Evaluation of Vortex Suppressors, Hydraulic Performance of Single Outlet Sumps and Sensitivity of Miscellaneous Parameters," ARL Report No. 49A-82.

28. Regulatory Guide 1.82 "Sumps for Emergency Core Cooling and Containment Spray Systems," U.S. Atomic Energy Commission, June 1974.

29. Letter, Bechtel Power Corporation to SNUPPS, BLSE 10,920 Dated August 19, 1982. Subject: Input Parameters for Hydraulic Model Studies of the Containment Sump.

30. Letter, Bechtel Power Corporation to SNUPPS, BLSE 11522 Dated 1-20-83, Subject: Draft Test Report - Model Testing of Containment Recirculation Sumps.